Contemporary Analysis and Numerical Simulation of Revisited Long-Term Creep Tests on Reinforced Concrete Beams from the Sixties

Tim Van Mullem(✉), Nicky Reybrouck, Pieterjan Criel, Luc Taerwe, and Robby Caspeele

Magnel Laboratory for Concrete Research,
Department of Structural Engineering, Ghent University, Ghent, Belgium
Tim.VanMullem@UGent.be

Abstract. The stresses and deformations in concrete change over time as a result of the creep- and shrinkage deformations of concrete. Different material models are available in literature in order to predict this time-dependent behaviour. These material models mostly have been calibrated on large datasets of creep specimens. In order to verify the accuracy of the contemporary material models with respect to the prediction of the creep behaviour of reinforced concrete beams, a cross-sectional calculation tool which employs the age-adjusted effective modulus has been developed and used to analyse an original set of 4 year-long creep data on reinforced beams from the 1960's. Six commonly used material models for the prediction of creep and shrinkage are considered in the current investigation: CEB-FIP Model Code 1990–1999, *fib* Model Code 2010, the model of EN1992-1-1, model B3, the Gardner Lockmann 2000 model, and ACI 209. The data on reinforced beams relates to an experimental investigation in collaboration with six major research institutes in Belgium. From 1967 until 1972 thirty-two reinforced beams with different reinforcement ratios were subjected, up until 4.5 years, to different stress levels in a four point bending configuration with a span of 2.8 m. In this paper a comparison between the measurements and the calculated deflections and strains is reported. Further, the deflections were also predicted using the contemporary creep models in combination with the nonlinear creep correction factor provided in EN1992-1-1, since the maximum concrete stresses in the beams were outside the service stress range of each of the models. Correcting for the nonlinearity of the creep coefficient significantly improves the calculated deflections. The most accurate predictions of the deflections at early age were obtained by the model of *fib* Model Code 2010. The Gardner Lockmann 2000 model exhibits the highest accuracy with respect to deflections at the end of loading and with respect to the creep rate.

1 Introduction

Concrete is an aging linear viscoelastic material. Under sustained loading, it undergoes a time–dependent deformation, on top of the elastic deformation, as a result of creep and shrinkage of the concrete. Creep and shrinkage influence each other. However, it is

D.A. Hordijk and M. Luković (eds.), *High Tech Concrete: Where Technology and Engineering Meet*, DOI 10.1007/978-3-319-59471-2_318

common practice to assume them to be independent and additive (Neville et al. 1983). While the creep phenomenon is well known, still no universally accepted creep theory has been formulated. That an accurate prediction of the time–dependent behaviour is required, is illustrated by the failure of the Koror–Babeldaob bridge in Palau. The failure of this bridge is partly attributed to a faulty execution of a retrofit which was required because of the underestimation of the long–term deflection, as a result of an inaccurate creep design (Bažant et al. 2011).

In order to take the creep and shrinkage behaviour into account different material models have been proposed in literature. These have been calibrated on large datasets which contain mostly data on small specimens without reinforcement. Hence, it is relevant to investigate whether these contemporary models are able to describe the time-dependent behaviour of reinforced concrete beams.

In order to investigate this aspect, experimental data from an extensive Belgian research programme was used, in which the time-dependent behaviour of concrete was studied. This extensive research programme consisted in a first phase, from 1967 until 1972, of experiments on reinforced concrete beams. From 1975 until 1980 also pre-stressed concrete beams were investigated and in a final phase, from 1981 until 1985, also partially prestressed concrete beams were investigated. In total six different Belgian universities participated in this programme: Ghent University, Vrije Universiteit Brussel, Université libre de Bruxelles, University of Leuven, Université Catholique de Louvain, and Université de Liège.

This paper revisits the results obtained from the tests on reinforced concrete beams. Reybrouck et al. (2015) performed already a preliminary analysis on these beams by only taking into account the model of EN 1992-1-1. In this contribution, the measured deflection and the measured strain (close to the most compressed fibre) at mid-span were compared against calculated values using six different material models. The considered models were: CEB-FIP Model Code 1990–1999, (CEB 1999), designated as MC90-99; *fib* Model Code 2010 (CEB-FIP 2013), designated as MC2010; the model of EN1992-1-1 (EN 1992-1-1 2004), designated as EC2; model B3 (Bažant and Baweja 2000), designated as B3; the Gardner Lockmann 2000 model (Gardner 2004), designated as GL 2000; and ACI 209 (ACI Committee 209 2008), designated as ACI.

2 Test Procedure

Four different types of reinforced concrete beams were tested, each with a different reinforcement ratio, see Fig. 1. All four types had a rectangular cross-section of 150 mm by 280 mm. They were all made out of concrete with the same composition. All the coarse aggregates, the sand, the cement and the main reinforcement were ordered at the same time and were then distributed over the laboratories. The steel quality of the longitudinal reinforcement was BE400S. The target mean compressive strength at 28 days on cubes with a side length of 200 mm was 35 MPa.

The long-term tests started at an age of 28 days in an air-conditioned room with a

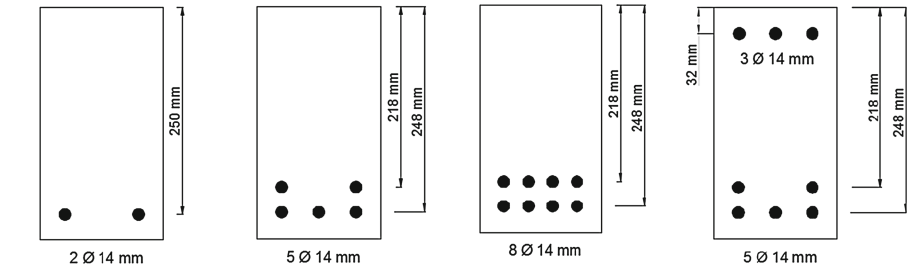

Fig. 1. Cross-section of the four different reinforced concrete beam types.

temperature of 20 °C ± 1 °C and a relative humidity of 60% ± 5%. The beams were subjected to a four point bending loading in pairs, see Fig. 2. The span was equal to 2.8 m. The beams were first loaded until the theoretical service load, upon which they were unloaded. Consecutively, they were immediately loaded again until the theoretical service load. The load was then further increased in steps of approximately 5% of the theoretical failure load up to 40–60% (depending on the beam type), 70%, 80%, or 90% of the observed failure load obtained from static tests on identical beams tested at an age of 28 days. This loading is much higher than the service load prescribed in design codes, nevertheless some of the loading values could occur in older buildings or buildings that are retrofitted. Note that the pair of beam type III loaded at the highest load failed during testing. These two beams were not taken into account in the analysis. In total 32 beams were tested under long-term loading for a period of maximum 4.5 years. In order to keep the loading constant throughout the entire testing period the hydraulic jacks were connected to accumulation vessels.

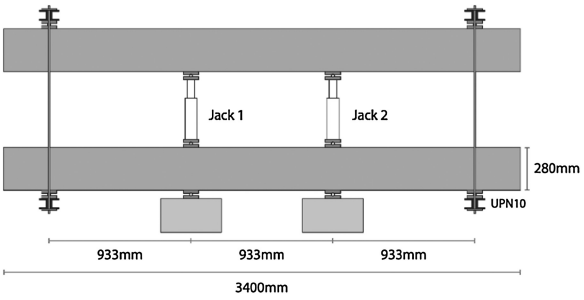

Fig. 2. Test setup for the long-term tests (Reybrouck et al. 2015).

3 Cross-Sectional Calculation Method

The predictions of the time–dependent deformations according to the different material models were calculated using a cross–sectional method as described in Ghali et al. (2002). Under the assumption of a linear elastic relationship between stresses and

strains, the instantaneous strain ε_O and curvature ψ at a reference point O can be calculated by:

$$\begin{bmatrix} \varepsilon_O \\ \psi \end{bmatrix} = \frac{1}{E_{ref} \cdot (A \cdot I - S^2)} \cdot \begin{bmatrix} I & -S \\ -S & A \end{bmatrix} \cdot \begin{bmatrix} N_{eq} \\ M_{eq} \end{bmatrix} \quad (1)$$

with E_{ref} a reference modulus of elasticity which is taken equal to the modulus of elasticity of concrete measured at 28 days, N_{eq} and M_{eq} the equivalent normal force and moment on the cross–section, and with A, S, and I respectively the transformed area of the cross-section, the transformed static moment about an axis through O, and the transformed moment of inertia about an axis through O. For a beam subjected to simple bending there is no external normal force. Hence, N_{eq} needs to be put equal to zero in Eq. (1).

Due to creep and shrinkage there will be a stress redistribution in the reinforced concrete element which causes a change of the strain and curvature: $\Delta\varepsilon_0$ and $\Delta\psi$. Assuming that these deformations are restrained by an artificial axial force ΔN and an artificial moment ΔM applied in the reference point O, the changes of the strain and curvature can then be calculated using Eq. (1), by replacing N_{eq} and M_{eq} by ΔN and ΔM. The restraining forces are not applied immediately at full strength but develop over time due to the time-dependent character of creep and shrinkage. Thus E_{ref} needs to be replaced by the age–adjusted effective modulus $\overline{E}_c(t, t_0)$, and similarly A, S, and I need to be replaced by their age–adjusted counterpart. The age–adjusted effective modulus can be calculated according to the equation proposed by Bažant (1972):

$$\overline{E}_c(t, t_0) = \frac{E_c(t_0)}{1 + \chi(t, t_0) \cdot \varphi(t, t_0)}$$

where $E_c(t_0)$ is the instantaneous modulus of elasticity at time of loading t_0, $\varphi(t, t_0)$ is the creep coefficient according to one of the material models and $\chi(t, t_0)$ is an aging coefficient. The calculation of the aging coefficient is computationally intensive. However, the aging coefficient can at first instance be assumed to be constant and equal to 0.8. Note that the deflections were also computed using a calculated aging coefficient and it was observed that this had an almost unnoticeable influence on the results.

All reinforced beams exhibited cracking under the applied loading. When the beams were cracked, the strain and curvature were calculated by considering the tension– stiffening effect (Ghali et al. 2002) in order to take into account the contribution of the concrete in the tension zone to the stiffness of the beams.

Once the strain and curvature in the reference point are known, the strain in any fibre of the cross-section can be calculated. The deflection of the beams is derived from the curvature over the length of the beam using the principle of elastic weights.

When the stresses become too high, the linear creep coefficient proposed in the different material models is no longer valid because the creep becomes nonlinear. In order to take the nonlinearity into account, the equation available in EN 1992-1-1 (2004) was used. To do so the linear creep coefficient $\varphi(\infty, t_0)$ for all models was replaced by a nonlinear creep coefficient $\varphi_k(\infty, t_0)$:

$$\varphi_k(\infty, t_0) = \varphi(\infty, t_0) \cdot \exp(1.5 \cdot (k_\sigma - 0.45)) \quad (2)$$

in which k_σ is the stress–strength ratio $\sigma_c / f_{ck}(t_0)$, where σ_c is the compressive stress in the studied fibre and $f_{ck}(t_0)$ is the characteristic concrete compressive stress at t_0. This correction was only applied for the part of the cross–section which surpassed the limit value of $0.45 f_{ck}(t_0)$. EN 1992-1-1 (2004) considers this limit value to be the boundary of linear creep but does not describe a maximum stress value up to which this correction factor can be used. MC2010 (CEB-FIP 2013) proposes a similar equation with a validity stress range between 0.4 and 0.6 of the mean concrete strength at the moment of loading. Some beams had a stress outside this validity range. The performed analysis indicates the appropriateness of correcting the creep coefficient, but new correction factors should be developed for highly stressed concrete.

4 Results

For each reinforced concrete beam the deflection at mid-span was calculated six times according to the six different material models using the cross-sectional method described above. As an example, Fig. 3 shows the comparison between measured and calculated deflections for three of the beams of type II. The calculated deflections have been computed using a linear creep coefficient; thus without the application of Eq. (2). It can be seen that prior to the application of the load at 28 days, the beams showed a small deflection as a result of restrained shrinkage. At the moment of load application the calculated instantaneous deformation agrees well with the measurements, although it is slightly underestimated for the beam loaded at 90% of the failure load. However, all the models underestimate the time–dependent deformation. Furthermore, the underestimation increases in function of the applied load.

When analysing the strains, a similar trend can be found as for the deflections. The calculated strains for the beams loaded at a lower level are reasonably accurate, although the difference between the measured and calculated values increases over time. For the beams subjected to the higher load levels, the strains are significantly underestimated, as can be seen in Fig. 4. Due to the linear elastic relationship which was assumed between the stress and the strain in the calculations, the calculated strains are proportional to the load level. The difference between the calculated strains of for example the beams loaded at 70% and 80% is the same as the difference between the beams loaded at 80% and 90%, as can be seen in Fig. 4. The tested beams did not exhibit this linear behaviour. The assumption of a linear elastic relationship between stress and strain is only valid for lower stress and strain levels, explaining why the higher loaded beams are so severely underestimated.

Calculations showed that in most of the beams the stress in part of the cross-section was outside the service stress range. EN 1992-1-1 (2004) prescribes $0.45 f_{ck}(t_0)$ as the limit stress for linear creep. Every model has a slightly different limit stress for linear

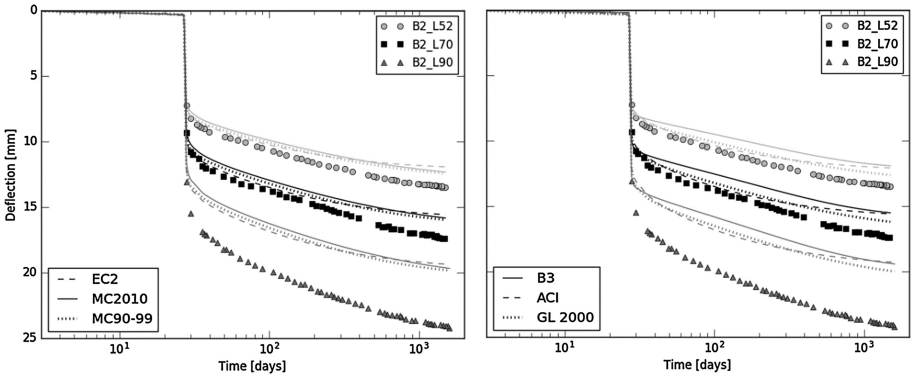

Fig. 3. Calculated (continuous lines) and measured (dots) deflections at mid–span for the beams of type II loaded at respectively 52%, 70% and 90% of the observed failure load.

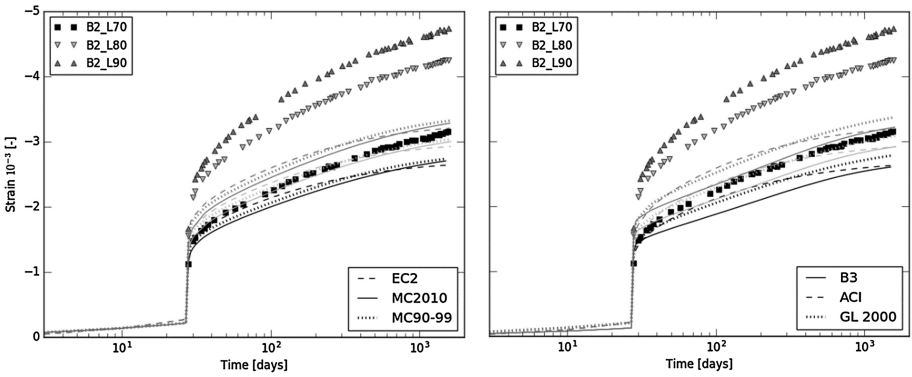

Fig. 4. Calculated (continuous lines) and measured (dots) compressive strains (at 8 mm below most compressed fibre) at mid-span for the beams of type II loaded at resp. 70%, 80% and 90% of the observed failure load.

creep. However, the stresses were so high that they surpassed the limit stress of all the models. In order to accommodate for this observation, the deflections calculated according to the different models were recalculated using the nonlinear creep correction factor, see Eq. (2). The use of this correction factor significantly improved the predictions, as is illustrated for some models in Fig. 5. Similar results can be obtained for the other models. Despite the improvement the models still underestimate the deflection of the beam subjected to the highest load level.

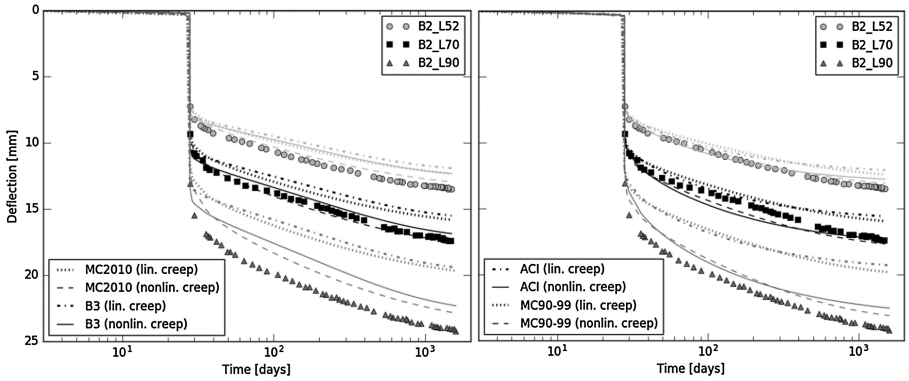

Fig. 5. Comparison between calculated deflections at mid-span with and without the use of a nonlinear creep correction factor.

5 Discussion

For those cases where the nonlinearity of the creep is not accounted for, the models still predict the time–dependent behaviour of the beams subjected to the lower load levels reasonably well. For the beams subjected to the higher load levels, the models underestimate the time-dependent behaviour, resulting in an increased difference between the measured and the calculated values over time.

The underestimation of the deflections and the strains are partly explained by the fact that the linear relationship which was assumed between the stress and the strain is no longer valid at higher load levels. The material models are also calibrated on data in the service stress range. It has been shown that most of the beams in this dataset are outside of this service stress range. Therefore, the material models may no longer be valid which results in higher inaccuracies.

The deflection at the end of the loading period is most accurately calculated by GL 2000, followed by MC90-99 and MC2010. The creep rate at a later age (between 119 days of loading and the end of loading) is predicted most accurately by B3, followed by GL 2000 and MC2010. Note that at an early age (up to 119 days of loading) ACI most accurately predicts the deflection.

When using the nonlinear creep correction, the accuracy of the calculated deflections is substantially increased. However, near the end of loading the deflection is on average still underestimated. At an early age (up to 119 days of loading) MC2010 calculates the deflection the most accurately, while the creep rate is most accurately calculated according to GL 2000. At the end of loading the deflection is most accurately calculated by GL 2000, followed by MC90-99 and MC2010. The creep rate at a later age (between 119 days of loading and the end of loading) is predicted equally accurate by B3 and GL 2000, followed by MC2010.

6 Conclusion

Under the assumption of an elastic relationship between stress and strain, the studied models are able to predict the deflection and the compressive strain accurately, as long as the stress is inside the service stress range. When the stress is outside the service stress range, creep becomes nonlinear. The deflection and the strain are then significantly underestimated by the material models. The application of the proposed nonlinear creep correction factor improves the calculated deflections of the studied models with respect to the available data on reinforced beams. It should be investigated if the method can be further improved. By using this method the deflections at the end of loading are most accurately calculated by GL 2000, followed by MC90-99 and MC2010. The creep rate calculated over the entire testing period is most accurately calculated by GL 2000.

References

ACI Committee 209: ACI Report 209.2R-08: Guide for Modeling and Calculating Shrinkage and Creep in Hardened Concrete: American Concrete Institute (2008)

Bažant, Z.P.: Prediction of concrete creep effects using age-adjusted effective modulus method. J. ACI **69**, 212–217 (1972)

Bažant, Z.P., Baweja, S.: Creep and shrinkage prediction model for analysis and design of concrete structures: model B3. Paper presented at the Adam Neville Symposium: Creep and Shrinkage—Structural Design Effects, Michigan, USA (2000)

Bažant, Z.P., Hubler, M.H., Yu, Q.: Pervasiveness of excessive segmental bridge deflections: wake-up call for creep. ACI Struct. J. **108**(6) (2011). doi:10.14359/51683375

CEB-FIP: fib Model Code for Concrete Structures 2010. Wiley, New York (2013)

CEB: Structural Concrete - Textbook on Behaviout, Design and Performance. Updated Knowledge of the CEB/FIP Model Code 1990 *fib Bulletin 2*. Lausanne, Switzerland: Federation Internationale du Beton (1999)

EN 1992-1-1: Eurocode 2: Design of concrete structures. Part 1-1: General – common rules for buildings and civil engineering structures. British Standards Institution, London (2004)

Gardner, N.J.: Comparison of prediction provisions for drying shrinkage and creep of normal-strength concretes. Can. J. Civil Eng. **31**(5), 767–775 (2004)

Ghali, A., Favre, R., Elbadry, M.: Concrete Structures: Stresses and Deformations. Spon Press, New York (2002)

Neville, A.M., Dilger, W.H., Brooks, J.J.: Creep of Plain and Structural Concrete. Longman Inc., New York (1983)

Reybrouck, N., Criel, P., Caspeele, R., Taerwe, L.: Modelling of long-term loading tests on reinforced concrete beams. Paper presented at the CONCREEP 10 Conference, Vienna, Austria (2015)